

Genome-wide Loss of Heterozygosity Analysis from Laser Capture Microdissected Prostate Cancer Using Single Nucleotide Polymorphic Allele (SNP) Arrays and a Novel Bioinformatics Platform dChipSNP^{1,2}

Marshall E. Lieberfarb,³ Ming Lin,³ Mirna Lechpammer, Cheng Li, David M. Tanenbaum, Phillip G. Febbo, Renée L. Wright, Judy Shim, Philip W. Kantoff, Massimo Loda, Matthew Meyerson, and William R. Sellers⁴

Departments of Medical Oncology [D. T., P. G. F., J. S., P. W. K., M. M., W. R. S.], Radiation Oncology [M. E. L.], and Biostatistical Sciences [C. L.], Dana-Farber Cancer Institute; Departments of Medicine [P. W. K., W. R. S.] and Pathology [M. Lec., M. Lod.], Brigham and Women's Hospital; Departments of Medicine [P. G. F., P. W. K., W. R. S.] and Pathology [M. Lod., M. M.], Harvard Medical School; and Department of Biostatistics [M. Lin, C. L.], Harvard School of Public Health, Boston, Massachusetts 02115

Abstract

Oligonucleotide arrays that detect single nucleotide polymorphisms were used to generate genome-wide loss of heterozygosity (LOH) maps from laser capture microdissected paraffin-embedded samples using as little as 5 ng of DNA. The allele detection rate from such samples was comparable with that obtained with standard amounts of DNA prepared from frozen tissues. A novel informatics platform, dChipSNP, was used to automate the definition of statistically valid regions of LOH, assign LOH genotypes to prostate cancer samples, and organize by hierarchical clustering prostate cancers based on the pattern of LOH. This organizational strategy revealed apparently distinct genetic subsets of prostate cancer.

Introduction

Progress in treating human prostate cancer has been hampered by the finding that histologically identical cancers exhibit widely variant clinical behavior. It is anticipated that the development of molecular taxonomies of prostate cancer will lead to the definition of unique cancer subsets each marked by different clinical behavior, probabilities of response to therapy, and cancer biology. Genomic efforts to render such molecular classifications have included expression profiling, proteome analysis, and comparative genomic hybridization. These technologies typically require nonfixed cancer tissue and often substantial quantities of cancer tissue. Ultimately, the widespread clinical use of cancer classification methods will require technologies capable of assaying small foci of cancerous tissue isolated from paraffin-embedded tissues. Such technologies would be widely applicable not only to routine clinical care but also to the retrospective analysis of existing large paraffin-embedded sample collections obtained during clinical trials or from large population-based cohorts. Such data sets have largely been unstudied by current technologies.

Recessive oncogenic alterations typically lead to the biallelic inactivation of tumor suppressor genes (1). Alterations such as homozygous and heterozygous deletions or gene conversions are thought to be among the most common genetic abnormalities in epithelial cancers

and the detection using LOH⁵ analysis as being essential to the discovery of the genes targeted by such events (2). Oligonucleotide microarrays, capable of simultaneously determining the genotype of 1494 SNPs, have been used to map regions of LOH in small cell lung, breast, bladder, and prostate cancer (3–7). In small cell lung cancer, detection of regions of LOH using SNP arrays was shown to be comparable with LOH detection using microsatellite markers but required cancer cell purity of $\geq 90\%$ (3). Similarly, LOH events detected by SNP arrays in bladder cancer were consistent with microsatellite-detected events (6). Here, we show that using this technology, the genotype of 1494 SNP alleles and genome-wide SNP-based LOH maps can be obtained from laser capture microdissected samples using as little as 5 ng of DNA obtained from paraffin-embedded prostate cancer samples. Furthermore, we demonstrate the utility of a new bioinformatic tool, dChipSNP, that automates the detection of shared regions of LOH, allows for the hierarchical clustering of cancers based on patterns of shared LOH, and allows the analysis of the relationship between clinical parameters and LOH genotypes. Using these methods, we show that subtypes of prostate cancer likely arise through independent genetic pathways.

Materials and Methods

Prostate Cancer Samples and Clinical Data. Paraffin blocks along with frozen SVs were available for 50 of a set of 52 prostate cancer samples, the clinicopathological characteristics of which were described previously (8).

DNA Isolation. Half of each snap-frozen SV sample was fixed in 10% buffered Formalin acetate, mounted in Tissue-Tek OCT, H&E stained, and visualized by light microscopy to confirm the absence of cancer. Germ-line DNA was prepared from the remainder by proteinase K digestion in SDS buffer followed by two extractions in Tris-buffered phenol and chloroform extraction. DNA was precipitated with 1/10th volume of 3.5 M sodium acetate, 20 μg of glycogen, and 2.5 volume of ethanol; washed in 70% ethanol twice; and resuspended in 50 μl of TE.

Cancer DNA was obtained from the corresponding formaldehyde-fixed paraffin-embedded prostatectomy cancer tissue. In brief, cancer epithelial cells were identified by pathologists (M. Loda and M. Lechpammer) and retrieved by LCM using an Arcturus PixCell II system (Mountain View, CA). Before DNA extraction, LCM adhesive caps were visualized by light microscopy to ensure $\geq 90\%$ purity of epithelial cells. Cancer cells adhered to the LCM cap were incubated in 50 μl of digestion buffer (1% Tween 20, 1 mg/ml Proteinase K, and $1 \times \text{TE}$) overnight at 37°C, heated to 95°C for 10 min, and clarified by centrifugation. DNA was quantified using the PicoGreen double-stranded DNA Quantitation Kit using 2 μl of DNA (Molecular Probes; P-11495). The sample volume was split in two and subjected to SNP PCR amplification according to the manufacturer's protocol without further DNA purification.

Received 6/11/03; accepted 6/30/03.

The costs of publication of this article were defrayed in part by the payment of page charges. This article must therefore be hereby marked *advertisement* in accordance with 18 U.S.C. Section 1734 solely to indicate this fact.

¹ Supported by the Damon-Runyon Lilly Clinical Investigator Award, National Cancer Institute (P50CA09038 and U01CA84995), Association for the Cure of Cancer of the Prostate, and Linda and Arthur Gelb Center for Translational Research. M. M. was supported by the Flight Attendant Medical Research Institute, the Pew Scholars in the Biomedical Sciences, and the National Cancer Institute (U01CA84995).

² Supplementary data for this article are available at Cancer Research Online (<http://cancerres.aacrjournals.org>).

³ M. E. L. and M. L. contributed equally to this work.

⁴ To whom requests for reprints should be addressed, Dana-Farber Cancer Institute, Boston, MA 02115. Phone: (617) 632-4750; Fax: (617) 632-5417; E-mail: william_sellers@dfci.harvard.edu.

⁵ The abbreviations used are: LOH, loss of heterozygosity; LCM, laser capture microdissection; SSPE, saline-sodium phosphate-EDTA; SNP, single nucleotide polymorphic allele; SV, seminal vesicle.

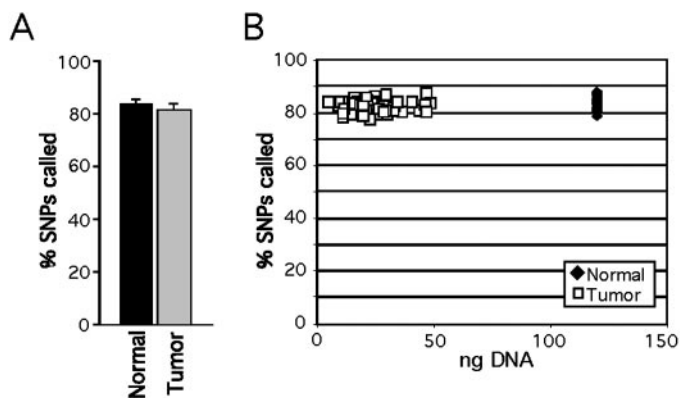


Fig. 1. High-quality SNP array data obtained from laser capture microdissected cancer cells. *A*, the average SNP allele call rate obtained from DNA extracted from flash-frozen noncancerous tissue or from DNA extracted from laser capture microdissected paraformaldehyde fixed, paraffin-embedded cancer cells. *B*, the relationship between DNA quantity and SNP call rate. DNA from cancer or normal samples (as described above) was quantified by PicoGreen measurement. DNA (120 ng) from each normal SV sample and 50% of the total available cancer DNA were used in the standard HuSNP protocol.

HuSNP PCR Amplification. Normal and cancer DNA was assayed using a modification of the GeneChip HuSNP protocol (Affymetrix). The total amount of input DNA was 120 ng for normal DNA and ranged from 4.4 to 47.1 ng (mean 26.4 ng) for cancer samples. For each genotype, 24 separate pools of primer pairs (~50–60 loci/pool) were added to 5 ng of normal DNA (or 0.37 pg to 2 ng of cancer DNA), 5 mM MgCl₂, 0.5 mM deoxynucleoside triphosphates, 1.25 units of AmpliTaq Gold (Applied Biosystems), and supplied buffer to a final reaction volume of 12.5 μl/pool. PCR amplification was carried out by denaturing at 95°C for 5 min, followed by 30 cycles of 95°C for 30 s, 58°C for 55 s, 72°C for 30 s, and a final extension of 7 min at 72°C. A 1-μl sample of each PCR reaction pool was diluted separately in 999 μl of H₂O. From each of these dilutions, 2.5 μl were removed and added to 0.8 μM biotinylated-T3 and 0.8 μM biotinylated-T7 primers, 4 mM MgCl₂, 0.4 mM deoxynucleoside triphosphates, 2.5 units of AmpliTaq Gold, and the supplied buffer for a final reaction volume of 25 μl and reamplified by denaturing at 95°C for 8 min, followed by 40 cycles of 95°C for 30 s, 55°C for 90 s, 72°C for 30 s, and a final extension of 7 min at 72°C. Successful PCR amplification was confirmed by resolving 1.8 μl of each pool in a 3% agarose gel. The 24 pools were combined and concentrated in a Microcon-YM10 centrifugal filter (Millipore Corp.), and the final sample volume was adjusted to 60 μl.

Hybridization, Washing, and Staining of the HU2K Oligonucleotide Array. Thirty microliters of each sample were diluted in 3 M Tetramethylammonium chloride, 2 nM oligonucleotide B1 (Affymetrix), 10 mM Tris-HCl (pH 7.8), 0.01% Tween 20, 5 mM EDTA (pH 8.0), 100 μg/ml herring sperm DNA, and 5 × Denhardt's solution to a final volume of 135 μl; heated to 95°C for 10 min; and quenched on ice for 5 min. Samples were then hybridized to the GeneChip HuSNP arrays (Affymetrix) overnight at 44°C at 40 rpm. Arrays were washed twice with 6 × SSPE, 0.01% Triton X-100 at 25°C, six times with 4 × SSPE, 0.01% Triton X-100, and stained with 500 μl of 50 μg/ml R-Phycoerythrin Streptavidin (Molecular Probes), 5 μg/ml biotinylated-anti-streptavidin antibody (Vector Labs), in 6 × SSPE, 1 × Denhardt's solution, and 0.01% Triton X-100 for 30 min at 25°C. The arrays were washed six times with 6 × SSPE, 0.01% Triton X-100 at 25°C.

Scanning of the HuSNP Arrays and Assigning Genotypes. After staining of the arrays, the chips were scanned using a HP GeneArray Scanner according to the GeneChip HuSNP Mapping Assay Manual (Affymetrix). Genotypes were assigned by the Affymetrix GeneChip 4.0 software. For each SNP, possible assigned genotypes included, homozygous for one allele (AA or BB), heterozygous (AB). If the software could not make a genotype determination, possible assignments included: (a) AB_A (implying the genotype is either AB or A); (b) AB_B (indicating the genotype is either AB or B); or (c) "no signal." The overall call rate was determined by the software to the number of SNPs assigned to AB, AA, or BB divided by the total number of SNPs on the microarrays (1494).

dChipSNP Analysis. The detailed statistical methods used to define regions of LOH, assign LOH calls to each cancer, and cluster cancers based on

LOH are discussed and presented in full in a forthcoming study.⁶ Briefly, within a 6 Mb window, a summary LOH score was derived across the entire set of cancer/normal comparisons. The summary LOH score was compared with the same score calculated from randomly permuted data. Regions of LOH differing statistically in the actual data from that derived from the permuted data were identified, and LOH assignments were made for each cancer based on the calls made for specific SNP alleles within the bounded region. Hierarchical clustering based on LOH calls for these specific regions was carried out as described previously (9).

Results and Discussion

Fifty-two prostate cancers, obtained at the time of radical prostatectomy, were studied previously by expression profiling to predict outcome after radical prostatectomy and detect the presence of an expression-based metastatic signature (8, 10). For each cancer, paired normal germ-line DNA was purified from pulverized unfixed frozen SV obtained at the time of surgery. Sections of each SV were examined histologically and found to be free of cancer.

The genotypes for 1494 SNPs were obtained using 120 ng of SV as the normal DNA. As described previously, each SNP allele was specifically amplified in 24 pooled highly multiplexed PCR reactions, and after reamplification and labeling, the genotype of each allele was determined by hybridization to the Hu2K SNP array (Affymetrix) using the standard HuSNP protocol (as described in Lindblad-Toh, 2000). The rate of alleles successfully called (call rate) on the array is an indicator of the quality of the DNA extraction, amplification, and hybridization procedures and determined using the MAS software (Affymetrix). The average call rate was 83.2% and ranged from 74.8 to 87.7% for assays run on the SV DNA. These results are consistent with data published previously (Fig. 1).

In parallel, paraffin-embedded cancer blocks were retrieved for each patient, sectioned, and reviewed by experienced prostate cancer pathologists (M. Loda and M. Lechpammer). Pure populations of malignant prostate epithelial cells were obtained using a Pixell LCM instrument. For each cancer, cells were collected onto the LCM cap until the cap was approximately half full. DNA was extracted in SDS-proteinase K buffer and used without further purification. Half of the LCM material, ranging from 4.6 to 47.1 ng of DNA, was then used in the SNP amplification protocol without further adjustment. SNP allele call rates in the cancer samples ($81.6 \pm 3.3\%$) did not vary significantly from that obtained with the normal DNA (Fig. 1). Thus, the quality of SNP genotyping with LCM-captured DNA was comparable with that obtained with DNA extracted by standard methods (Fig. 1). Using these methods, LOH detection was carried out in 50 available cancers from the original set of 52 cancers studied previously. The raw data are available on the Internet.⁷

To enable the analysis of the SNP array data across multiple cancer-normal comparisons, a new informatics platform known as dChipSNP was developed. This platform is based on dChip, a bioinformatics package for oligonucleotide array-based expression analysis (11, 12). The details of the statistical methods used in the dChipSNP program for LOH determination are described in a forthcoming study.⁵ dChipSNP integrates publicly available SNP, gene, and cytoband mapping information with automated methods for detecting statistically meaningful regions of LOH from a series of paired normal and cancer SNP genotypes. dChipSNP is available for download on the Internet.⁸

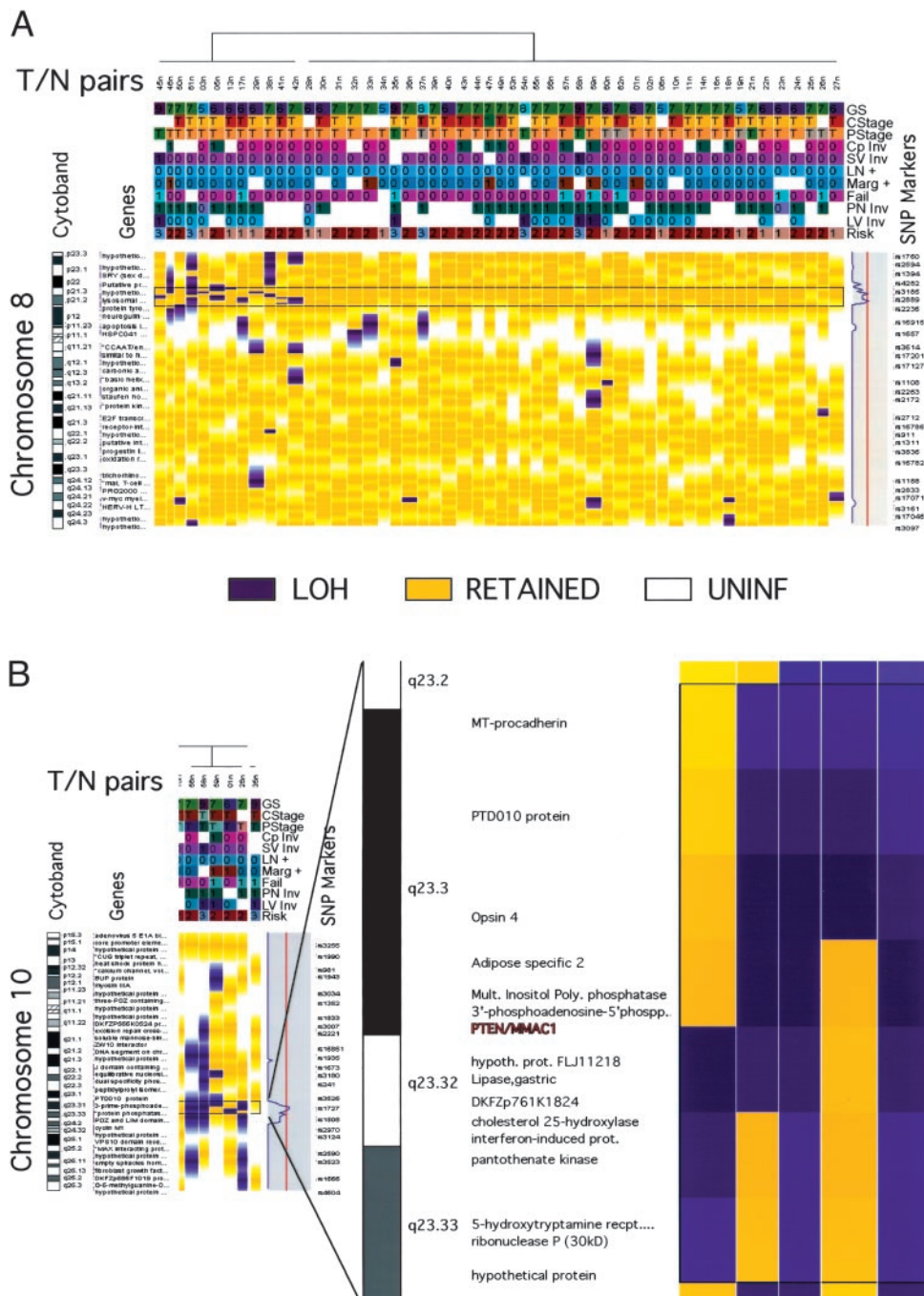
Regions of LOH, usually arising as a result of either hemizygous deletion or gene conversion events, are typically defined as stretches

⁶ M. Lin *et al.*, submitted for publication.

⁷ Internet address: <http://research.dfci.harvard.edu/sellerslab/datasets/index.html>.

⁸ Internet address: <http://www.dchip.org/>.

Fig. 2. SNP array-based LOH maps for 8p21 and 10q23. A, automated detection and demarcation of the 8p21 region of LOH in prostate cancers using dChipSNP. Each column represents one tumor/normal pair. Along the far right, the position and name of each SNP are shown. Where the density of SNPs is too high to allow a full display of all SNPs, hidden SNPs are indicated by small blue dots. Additionally along the right within the shaded gray box is the LOH score indicated as a blue line and the $P = 0.05$ threshold indicated as a red line. Tumors in which there is LOH within the 8p21 region are identified and organized by hierarchical clustering (left branch) as distinct from tumors with definitively retained alleles within the 8p21 regions (right branch). There are no uninformative tumors for this region. Finally, clinical or pathological information pertinent to each tumor is indicated along the top (GS, Gleason Score; CStage, Clinical Stage; PStage, Pathological Stage; Cp Inv, Capsule invasion; SV Inv, SV invasion, LN +, lymph node metastases; Marg +, surgical margin positive; Fail PSA, failure after prostatectomy; LV Inv, lymphatic vessel invasion; and risk, prostate cancer risk group). B, automated detection and demarcation of the 10q23 region of LOH. dChipSNP precisely demarcates the area centered over the PTEN tumor suppressor gene. Left panel, a segment of the LOH plot for chromosome 10 (as in Fig. 2A); however, only those tumors with LOH are shown. dChipSNP allows an expanded zoom in view, and this reveals that the segment of chromosome 10 identified precisely overlies the PTEN tumor suppressor gene.



of chromosomal areas where all heterozygous and thereby informative alleles are rendered homozygous in the cancer. The boundaries of such regions of LOH are defined by either the presence of retained heterozygous alleles, the ends of chromosomal arms, or the centromere. This classical definition assumes that all data points are completely accurate and that all polymorphic alleles are mapped correctly within the genome. Array-based methods of SNP detection may have a certain degree of inaccuracy (“noise”), and moreover, the precise genome mapping of each SNP is still not completely stable. Thus, “true” regions of LOH can be interrupted by apparently false positive “retained” SNP alleles. Conversely, true regions of retention of heterozygosity may be interrupted by false LOH calls. To take these concerns into consideration, a method for assessing the probability of LOH within a given set of normal cancer comparisons was used where

within a sliding 6 Mb window, a summary LOH score was derived. To determine whether the measured summary LOH scores exceed those that might occur by chance alone, 1000 data sets were generated in which the sample designation of cancer versus normal was randomly permuted. Regions of deletion were identified where the summary LOH score exceeded that found in the permuted data sets. A P -value, corrected for multiple hypothesis testing, of 0.05 was used as the cutoff (as described in detail in Lin *et al.*). The predicted region of LOH was demarcated by dChipSNP. Fig. 2A shows the application of this platform to this data set, specifically showing a demarcated region of deletion predicted on chromosome 8 (8p21).

In this manner, seven regions of significant LOH were found in a fully automated fashion, including 1p33–34, 3q27, 8p21, 10q23, 15q12 16q23–24, and 17p13 (Figs. 2, A and B and Supplemental Fig.

1, A–F). LOH in prostate cancer localized to 1p, 8p21, 10q23, 16q23, and 17p13 have all been reported previously by multiple investigators, with LOH of 8p21 being among the most frequently reported in prostate cancer (Refs. 13–27 and reviewed in Ref. 28). This methodology, given sufficient overlapping alterations, might lead to enhanced localization of putative genes targeted within the regions of LOH. The *PTEN* gene is thought to be the tumor suppressor gene targeted by alterations in the 10q23 cytoband. The density of informative SNPs in this region, while relatively low, was nonetheless sufficient to give a peak prediction of LOH that corresponded directly with the physical location of *PTEN* (Fig. 2B). Together, the detection of known regions of LOH and colocalization of a predicted peak with a known cancer suppressor argue that microarray-based LOH detection and the automated statistical methods developed for analyzing these data are robust.

Next, we sought to determine whether sample organization algorithms, such as hierarchical clustering, could be applied to this data set. Here, the direct use of the actual SNP allele data in clustering algorithms, much as one would use expression array data, would lead to sample organization based on the germ-line genetic similarities of the individuals rather than on the genetic similarities of the cancer. Moreover, LOH of the same chromosomal region can be marked by completely different sets of heterozygous and thus informative SNPs in distinct cancer–normal pairs. Thus, it is necessary to render the SNP data for each cancer–normal pair into an LOH-based data set. To this end, for each cancer–normal pair, a designation of LOH, retained or uninformative, was made based on the actual genotype of the heterozygous SNPs within the seven regions of significant LOH identified above. Here, retention (RET) was defined as the presence of an informative allele within the region of interest in which heterozygosity was retained (RET) without any heterozygous alleles showing LOH. In dChipSNP, these data can be output as specific tab delimited data sets (see Supplemental Table 1). For purposes of display only, the regions of LOH or retention for each cancer–normal pair are projected as a heat map of blue or yellow using a 50% extension to the next

nearest heterozygous SNP. In certain instances, the heat map extending from an allele showing LOH extends into the region of LOH; however, if the actual SNP allele is not within the demarcated region, then the cancer is not designated as LOH for that region.

After such designation, one can cluster cancers based only on a single region of LOH in the chromosome view (Fig. 2) or using all regions of loss defined as significant in the whole genome view. In the first instance, hierarchical clustering was driven by using the comparisons LOH-to-LOH, LOH-to-RET, and RET-to-RET. This resulted in either two or three clusters of tumors for each region of LOH, specifically a cluster with LOH, a cluster with retention, and a cluster of uninformative tumor (Fig. 2A and Suppl. Fig. 1, A–F). This analysis allows the automatic assignment of the genotype for this region to each individual tumor and can be then used in further downstream analysis pertinent to the specific region, *e.g.*, we have looked for gene expression signatures associated with specific regions of LOH by using those tumors that are definitely scored as LOH and those that are definitely scored as RET, while ignoring those that are uninformative in a given region.

For many human cancers, it is thought that there is a sequential progression of accumulated genetic events, ultimately culminating in a metastatic cancer. In prostate cancer, it remains to be seen whether the heterogeneous nature of the disease can be understood based on this model wherein early genetic events would be then accompanied or not accompanied by late genetic alterations, thus leading to differences in the disease, or whether an alternative, but not mutually exclusive, model in which distinct “parallel” sets of genetic alterations might occur, leading to unique genetic cancer subtypes that have distinct clinical behavior.

To determine whether genome-wide LOH mapping might provide an answer to this question, hierarchical clustering was used to look for separation or cosegregation of LOH events. In this analysis, clustering was enacted using the seven regions of LOH passing the $P = 0.05$ threshold. Again, each tumor was assigned a lost or retained designation based on SNP alleles within the boundaries of LOH. The

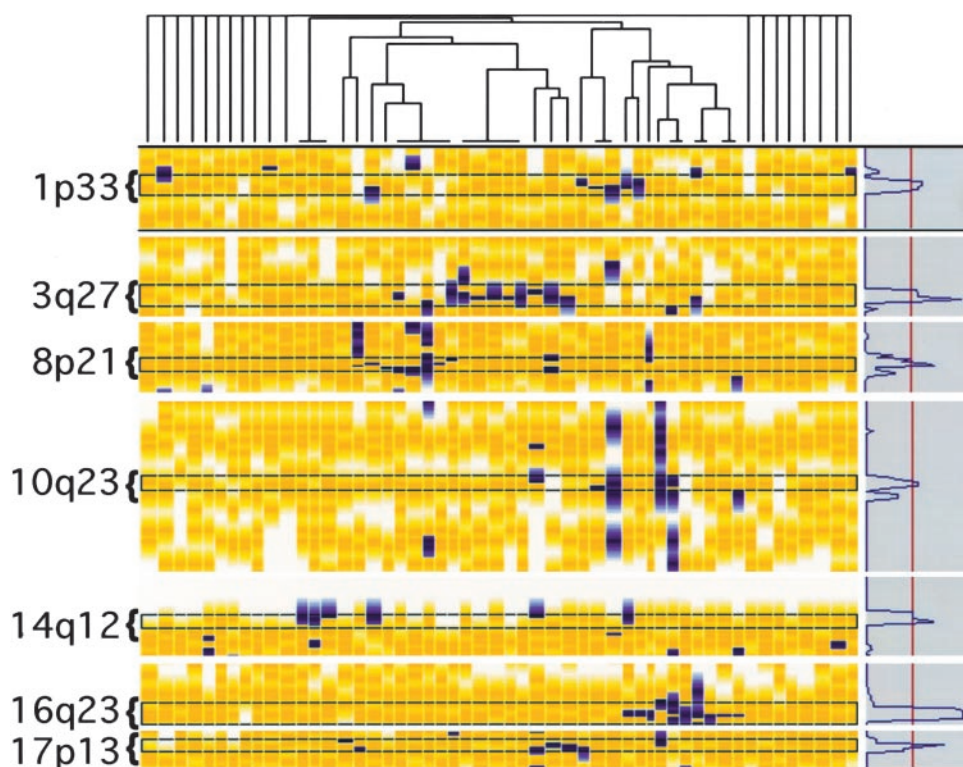


Fig. 3. Hierarchical clustering of prostate cancers based on LOH similarity. Each of the cancers was assigned a designation of RET, LOH, or uninformative for the seven regions of LOH detected in this data set. Hierarchical clustering of samples without clustering of regions was undertaken using the comparisons of LOH:LOH and LOH:RET, whereas RET:RET and uninformative loci were ignored. Tumor normal pairs are shown as columns, whereas the indicated regions of LOH and SNP alleles within them are shown as rows. Regions of LOH are indicated by blue, although regions of RET are indicated by yellow.

comparisons of LOH-to-LOH and LOH-to-RET were used, whereas RET-to-RET was ignored. This allows clustering to be driven primarily by the similarity or difference in a deletion rather than the similarity in retention.

A number of cancers had either no informative alleles or did not show LOH in any of the seven regions and thus were not clustered in this analysis (single branches in Fig. 3). The clustering of tumors with sufficient information revealed that samples were clustered into distinct branches and that these branches contained tumors enriched for specific nonoverlapping regions of heterozygosity. These data suggest the possibility that there are distinct genetic subsets of prostate cancer that can be defined based on LOH analysis. Validation of this observation on higher density and thus more sensitive SNP arrays is an important next step.

In summary, we provide a novel and robust tool for LOH detection. This informatics package and the automated detection of LOH will be a vital tool for the analysis of large SNP LOH data sets that will be available on the second generation of SNP arrays where the cancer-normal genotypes of >10,000 SNP alleles will be available.

Acknowledgments

We thank our colleagues in the Sellers and Meyerson Laboratories for their support and assistance in conducting this work.

References

1. Knudson, A. G., Jr. Mutation and cancer: statistical study of retinoblastoma. *Proc. Natl. Acad. Sci. USA*, 68: 820–823, 1971.
2. Cavenee, W. K., Dryja, T. P., Phillips, R. A., Benedict, W. F., Godbout, R., Gallie, B. L., Murphree, A. L., Strong, L. C., and White, R. L. Expression of recessive alleles by chromosomal mechanisms in retinoblastoma. *Nature (Lond.)*, 305: 779–784, 1983.
3. Lindblad-Toh, K., Tanenbaum, D. M., Daly, M. J., Winchester, E., Lui, W. O., Villapakkam, A., Stanton, S. E., Larsson, C., Hudson, T. J., Johnson, B. E., Lander, E. S., and Meyerson, M. Loss-of-heterozygosity analysis of small-cell lung carcinomas using single-nucleotide polymorphism arrays. *Nat. Biotechnol.*, 18: 1001–1005, 2000.
4. Schubert, E. L., Hsu, L., Cousens, L. A., Glogovac, J., Self, S., Reid, B. J., Rabinovitch, P. S., and Porter, P. L. Single nucleotide polymorphism array analysis of flow-sorted epithelial cells from frozen versus fixed tissues for whole genome analysis of allelic loss in breast cancer. *Am. J. Pathol.*, 160: 73–79, 2002.
5. Dumur, C. I., Dechsukhum, C., Ware, J. L., Cofield, S. S., Best, A. M., Wilkinson, D. S., Garrett, C. T., and Ferreira-Gonzalez, A. Genome-wide detection of LOH in prostate cancer using human SNP microarray technology. *Genomics*, 81: 260–269, 2003.
6. Hoque, M. O., Lee, C. C., Cairns, P., Schoenberg, M., and Sidransky, D. Genome-wide genetic characterization of bladder cancer: a comparison of high-density single-nucleotide polymorphism arrays and PCR-based microsatellite analysis. *Cancer Res.*, 63: 2216–2222, 2003.
7. Primdahl, H., Wikman, F. P., von der Maase, H., Zhou, X. G., Wolf, H., and Orntoft, T. F. Allelic imbalances in human bladder cancer: genome-wide detection with high-density single-nucleotide polymorphism arrays. *J. Natl. Cancer Inst. (Bethesda)*, 94: 216–223, 2002.
8. Singh, D., Febbo, P. G., Ross, K., Jackson, D. G., Manola, J., Ladd, C., Tamayo, P., Renshaw, A. A., D'Amico, A. V., Richie, J. P., Lander, E. S., Loda, M., Kantoff,

- P. W., Golub, T. R., and Sellers, W. R. Gene expression correlates of clinical prostate cancer behavior. *Cancer Cell*, 1: 203–209, 2002.
9. Eisen, M. B., Spellman, P. T., Brown, P. O., and Botstein, D. Cluster analysis and display of genome-wide expression patterns. *Proc. Natl. Acad. Sci. USA*, 95: 14863–14868, 1998.
10. Ramaswamy, S., Ross, K. N., Lander, E. S., and Golub, T. R. A molecular signature of metastasis in primary solid tumors. *Nat. Genet.*, 33: 49–54, 2003.
11. Schadt, E. E., Li, C., Ellis, B., and Wong, W. H. Feature extraction and normalization algorithms for high-density oligonucleotide gene expression array data. *J. Cell. Biochem. Suppl.*, 37: 120–125, 2001.
12. Li, C., and Hung Wong, W. Model-based analysis of oligonucleotide arrays: model validation, design issues and standard error application. *Genome Biol.*, 2: , 2001.
13. Lundgren, R., Kristofferson, U., Heim, S., Mandahl, N., and Mitelman, F. Multiple structural chromosome rearrangements, including del(7q) and del(10q), in an adenocarcinoma of the prostate. *Cancer Genet. Cytogenet.*, 35: 103–108, 1988.
14. Carter, B. S., Ewing, C. M., Ward, W. S., Treiger, B. F., Aalders, T. W., Schalken, J. A., Epstein, J. I., and Isaacs, W. B. Allelic loss of chromosomes 16q and 10q in human prostate cancer. *Proc. Natl. Acad. Sci. USA*, 87: 8751–8755, 1990.
15. Gray, I. C., Phillips, S. M., Lee, S. J., Neoptolemos, J. P., Weissenbach, J., and Spurr, N. K. Loss of the chromosomal region 10q23–25 in prostate cancer. *Cancer Res.*, 55: 4800–4803, 1995.
16. Sakr, W. A., Macoska, J. A., Benson, P., Grignon, D. J., Wolman, S. R., Pontes, J. E., and Crissman, J. D. Allelic loss in locally metastatic, multisampled prostate cancer. *Cancer Res.*, 54: 3273–3277, 1994.
17. Matsuyama, H., Pan, Y., Skoog, L., Tribukait, B., Naito, K., Ekman, P., Lichter, P., and Bergerheim, U. S. Deletion mapping of chromosome 8p in prostate cancer by fluorescence in situ hybridization. *Oncogene*, 9: 3071–3076, 1994.
18. MacGrogan, D., Levy, A., Bostwick, D., Wagner, M., Wells, D., and Bookstein, R. Loss of chromosome arm 8p loci in prostate cancer: mapping by quantitative allelic imbalance. *Genes Chromosomes Cancer*, 10: 151–159, 1994.
19. Bova, G. S., Carter, B. S., Bussemakers, M. J., Emi, M., Fujiwara, Y., Kyprianou, N., Jacobs, S. C., Robinson, J. C., Epstein, J. I., Walsh, P. C., *et al.* Homozygous deletion and frequent allelic loss of chromosome 8p22 loci in human prostate cancer. *Cancer Res.*, 53: 3869–3873, 1993.
20. Nupponen, N. N., Kakkola, L., Koivisto, P., and Visakorpi, T. Genetic alterations in hormone-refractory recurrent prostate carcinomas. *Am. J. Pathol.*, 153: 141–148, 1998.
21. Macoska, J. A., Powell, I. J., Sakr, W., and Lane, M. A. Loss of the 17p chromosomal region in a metastatic carcinoma of the prostate. *J. Urol.*, 147: 1142–1146, 1992.
22. Massenkeil, G., Oberhuber, H., Haillemariand, S., Sulser, T., Diener, P. A., Bannwart, F., Schafer, R., and Schwarte-Waldhoff, I. P53 mutations and loss of heterozygosity on chromosomes 8p, 16q, 17p, and 18q are confined to advanced prostate cancer. *Anticancer Res.*, 14: 2785–2790, 1994.
23. Deubler, D. A., Williams, B. J., Zhu, X. L., Steele, M. R., Rohr, L. R., Jensen, J. C., Stephenson, R. A., Changus, J. E., Miller, G. J., Becich, M. J., and Brothman, A. R. Allelic loss detected on chromosomes 8, 10, and 17 by fluorescence in situ hybridization using single-copy P1 probes on isolated nuclei from paraffin-embedded prostate tumors. *Am. J. Pathol.*, 150: 841–850, 1997.
24. Erbersdobler, A., Graefen, M., Wulbrand, A., Hammerer, P., and Henke, R. P. Allelic losses at 8p, 10q, 11p, 13q, 16q, 17p, and 18q in prostatic carcinomas: the impact of zonal location, Gleason grade, and tumour multifocality. *Prostate Cancer Prostatic Dis.*, 2: 204–210, 1999.
25. Elo, J. P., Harkonen, P., Kyllonen, A. P., Lukkarinen, O., Poutanen, M., Vihko, R., and Vihko, P. Loss of heterozygosity at 16q24.1-q24.2 is significantly associated with metastatic and aggressive behavior of prostate cancer. *Cancer Res.*, 57: 3356–3359, 1997.
26. Matsuyama, H., Pan, Y., Yoshihiro, S., Kudren, D., Naito, K., Bergerheim, U. S., and Ekman, P. Clinical significance of chromosome 8p, 10q, and 16q deletions in prostate cancer. *Prostate*, 54: 103–111, 2003.
27. Latil, A., Cussenot, O., Fournier, G., Driouch, K., and Lidereau, R. Loss of heterozygosity at chromosome 16q in prostate adenocarcinoma: identification of three independent regions. *Cancer Res.*, 57: 1058–1062, 1997.
28. Abate-Shen, C., and Shen, M. M. Molecular genetics of prostate cancer. *Genes Dev.*, 14: 2410–2434, 2000.